Development 133, 1035-1044 doi:10.1242/dev.02272

Semaphorin 3d guides laterality of retinal ganglion cell projections in zebrafish

Jill A. Sakai and Mary C. Halloran*

The optic chiasm is an important choice point at which retinal ganglion cell (RGC) axons either cross the midline to innervate the contralateral brain or turn back to innervate the ipsilateral brain. Guidance cues that regulate this decision, particularly those directing the midline crossing of contralateral axons, are still not well understood. Here we show that Sema3d, a secreted semaphorin expressed at the midline, guides the crossing of RGC axons in zebrafish. Both Sema3d knockdown and ubiquitous overexpression induced aberrant ipsilateral projections, suggesting that Sema3d normally guides axons into the contralateral optic tract. Live imaging in vivo showed that RGC growth cones responded to ubiquitous Sema3d overexpression by pausing for extended periods and increasing their exploratory behavior at the midline, suggesting that Sema3d overexpression causes the midline environment to become less favorable for RGC axon extension. Interestingly, Sema3d overexpression did not affect growth cone behaviors before the midline, suggesting that RGC axons normally respond to Sema3d only upon reaching the midline. After Sema3d knockdown, growth cones grew across the midline but then paused or repeatedly retracted, impairing their ability to leave the midline region. Our results indicate that a proper balance of Sema3d is needed at the midline for the progression of RGC axons from the chiasm midline into the contralateral optic tract.

KEY WORDS: Semaphorin, Axon guidance, Retinal ganglion cell, Optic chiasm, Zebrafish

INTRODUCTION

During development of the visual system, RGC axons extend from the eye to the midline of the ventral diencephalon, where the axon bundles cross to form the optic chiasm. From the chiasm, axons extend in the optic tract dorsally and caudally to the midbrain, where they form a retinotopic map on the surface of the optic tectum, the primary visual structure in lower vertebrates. The optic chiasm is an important guidance choice point at which RGC axons must choose between the contralateral and ipsilateral optic tracts. In fish and birds, all RGC axons cross the midline to innervate the contralateral side of the brain. However, in most animals with binocular vision, a subset of RGC axons turns back at the chiasm midline to project to the ipsilateral optic tectum.

Initial studies of RGC axon guidance at the chiasm identified the midline of the ventral diencephalon as a source of extrinsic guidance cues. Live imaging of mouse RGC growth cones showed behavioral differences between ipsilaterally and contralaterally projecting growth cones as they contacted midline tissue (Godement et al., 1994; Sretavan and Reichardt, 1993). In vitro, explants of midline tissue inhibited outgrowth from retinal cultures that normally gave rise to uncrossed axons, but did not affect explants that normally gave rise to crossed axons (Wang et al., 1995), suggesting that the midline tissue is selectively inhibitory to ipsilaterally projecting RGC axons. The chiasm region contains a population of cells that express the surface molecule CD44, which can affect the relative size of the crossed and uncrossed projections in mouse (Lin and Chan, 2003). Disruption of chondroitin sulfate proteoglycans, another family of cell-surface molecules expressed at the chiasm, reduced the uncrossed projection in mouse (Chung et al., 2000). EphrinB2 is also expressed at the midline and acts as a repulsive cue for axons that project ipsilaterally (Nakagawa et al., 2000). Together, these studies show that the midline tissue is a source of cues that help to determine the laterality of RGC projections. Interestingly, RGC axons in a zebrafish mutant lacking the Slit receptor Robo2 make ipsilateral errors in addition to other guidance errors (Hutson and Chien, 2002). However, this study and others in mice suggest that the main role of Slit/Robo signaling is to channel axons to the correct location of the optic chiasm rather than to provide laterality information (Erskine et al., 2000; Plump et al., 2002; Ringstedt et al., 2000).

Recent work indicates that the laterality decision is also regulated by intrinsic factors in RGCs. In mouse, the zinc-finger transcription factor Zic2 is expressed exclusively by ipsilaterally projecting RGCs, and is both necessary and sufficient for RGC axon repulsion by midline chiasm explants (Herrera et al., 2003). Zic2-positive RGCs also express the receptor tyrosine kinase EphB1, which appears to mediate repulsion from ephrinB2 at the midline to cause these axons to project ipsilaterally (Williams et al., 2003). Interestingly, *Xenopus* tadpoles lack retinal EphB1 and midline ephrinB2 expression, and have an entirely crossed retinal projection. During *Xenopus* metamorphosis, upregulation of ephrinB at the midline and EphB in a restricted part of the retina coincides with the development of an ipsilateral component of the visual pathway (Nakagawa et al., 2000). Together, these studies suggest that RGC axons project contralaterally unless otherwise specified to respond to repulsive cues at the midline. However, it is not yet clear what drives the large majority of RGC axons to cross the midline. Two winged helix transcription factors, Foxd1 and Foxg1, are expressed in complementary patterns in both retina and ventral diencephalon, and appear to be involved in development of the contralateral projection as mice deficient in either displayed increased ipsilateral projections (Herrera et al., 2004; Pratt et al., 2004). Another recent study showed that expression of the LIM-homeodomain transcription factor islet 2 is restricted to contralaterally projecting RGCs in mouse (Pak et al., 2004). However, no guidance cues at the midline have yet been shown to promote the crossing of RGC axons.

Neuroscience Training Program, and Departments of Zoology and Anatomy, University of Wisconsin, Madison, WI 53706, USA.

*Author for correspondence (e-mail: mchalloran@wisc.edu)

Accepted 4 January 2006

Here, we provide evidence that a secreted semaphorin, Sema3d, expressed at the chiasm guides the midline crossing of RGC axons in zebrafish. Zebrafish are an excellent system in which to study the development of the contralateral RGC projection, as all RGC axons cross the midline. Disruption of normal Sema3d through either global overexpression or knockdown induced aberrant ipsilateral projections without affecting other pathfinding decisions. Sema3d overexpression slowed or prevented RGC axon growth through the midline region, whereas Sema3d knockdown reduced the ability of RGC axons to leave the midline by increasing growth cone retraction in the optic tract. We propose that midline Sema3d is important for RGC axon extension from the chiasm midline into the contralateral optic tract.

MATERIALS AND METHODS

Animals

Zebrafish (*Danio rerio*) were maintained in a laboratory breeding colony on a 14 hour light/10 hour dark cycle. Embryos were maintained at 28.5°C and staged as described (Kimmel et al., 1995). Embryo age is defined as hours post-fertilization (hpf) or days post-fertilization (dpf). For live imaging experiments, embryos were kept in 0.003% 1-phenyl-2-thiourea after 22 hpf to block pigment formation. For heat induction, embryos were transferred to a 39°C water bath for one hour.

In situ hybridization and immunohistochemistry

A digoxigenin-UTP labeled riboprobe for *sema3d* was synthesized by in vitro transcription and hydrolyzed to an average length of 200-500 bases by limited alkaline hydrolysis (Cox et al., 1984). Whole-mount in situ hybridization was performed as described previously (Halloran et al., 1999). For double labeling, anti-acetylated tubulin (Sigma, St Louis, MO) at a dilution of 1:1000 was added to an overnight incubation in AP-tagged anti-digoxigenin antibody (Roche, Indianapolis, IN). Following the AP reaction, antibody labeling was completed with the Vectastain Mouse IgG ABC immunoperoxidase labeling kit (Vector Laboratories, Burlingame, CA).

For whole-mount immunohistochemistry, embryos were fixed in 4% paraformaldehyde for one hour at room temperature, treated with 0.1% collagenase (Sigma, St Louis, MO) in PBS, blocked in 5% sheep serum and 2 mg/ml BSA in PBS, and incubated in Zn-5 (Zebrafish International Resource Center, Eugene, OR) at a dilution of 1:500. Antibody labeling was completed with the Vectastain Mouse IgG ABC immunoperoxidase labeling kit (Vector Laboratories, Burlingame, CA).

Morpholino antisense

Morpholino oligonucleotides previously designed against the *sema3d* translation start site (Liu et al., 2004) were synthesized by Gene Tools (Corvallis, OR). The same sequence with four mismatched bases was used as a control. Morpholinos were diluted in Danieau buffer and 1% Phenol Red (Nasevicius and Ekker, 2000). RGC axon effects were seen using morpholino concentrations of 100-250 μM; higher concentrations caused high mortality and non-specific effects. For all experiments, approximately 1 nl of a 100-250 μM solution was injected into embryos at the one- to four-cell stage.

DiI injections and imaging

For axon labeling, embryos were mounted in 1% low-melting point agarose. A 0.5% solution of DiI (1,1′-dioctadecyl-3,3,3′,3′-tetramethylindocarbocyanine perchlorate, Molecular Probes, Eugene, OR) in dimethylformamide was pressure injected into the retina. For whole eye fills, embryos were fixed in 4% paraformaldehyde and dye was injected into multiple parts of the RGC layer and allowed to transport overnight. Confocal series were collected on a Zeiss Axiovert 100M microscope with the BioRad 1024 Lasersharp Confocal software package, and processed with Metamorph software (Universal Imaging Corporation, West Chester, PA).

For live imaging, small amounts of DiI were injected into ventronasal, nasal or dorsonasal retina and allowed to transport for one hour at room temperature. Timelapse movies were captured on a Nikon E600FN upright microscope with a Photometrix CoolSnapHQ camera at 28-30°C. For Sema3d overexpression experiments, a single *z*-plane was collected every minute for up to 14 hours. For Sema3d knockdown experiments, a *z*-stack of three to seven planes covering the extent of the growth cone was captured every two minutes for up to 23 hours.

Quantification of guidance errors

For quantification of the extent of ipsilateral tectal innervation, the tectal neuropil was outlined from a simultaneously imaged channel containing only autofluorescence. This tectal outline was overlaid onto reconstructions of confocal stacks of dorsally imaged RGC axon projections. A threshold was set for each image to match the distribution of visible projections, and the extent of ipsilateral innervation was determined as the percentage of tectal area over threshold. All analyses were performed blind to embryo treatment and groups were compared using two-tailed Student's *t*-tests.

For the identification of guidance errors in Sema3d morpholino-injected embryos, we analyzed confocal stacks of ventrally imaged DiI-labeled axons in the optic chiasm. Because Sema3d morpholino-injected embryos had reduced or absent tectal innervation when compared with control embryos, analysis was restricted to guidance errors visible in ventral views of the chiasm region. All analyses were performed blind to embryo treatment and groups were compared using binomial *z*-tests.

For analyses of live axon behaviors and growth rates, the distance between the eyes was divided into three regions: the 'midline region' was defined as the middle 20% of the intereye distance, spanning the chiasm midline; 'before midline' was defined as the region between the injected eye and the midline region; and 'after midline' was defined as the region between the midline region and the uninjected eye. Growth cone advance, retraction or pausing was recorded for each timelapse frame then analyzed by region. Overall axon growth rates were calculated for each region by measuring total distance traveled and total time spent in each region. Outgrowth was only measured in the first half of the 'after midline' region due to the dorsal turn of the optic projection medial to the contralateral eye. Groups were compared using two-tailed Student's *t*-tests.

RESULTS

sema3d is expressed at the midline of the optic chiasm during visual system development

The optic chiasm is formed by bundles of RGC axons crossing at the midline of the ventral diencephalon (Fig. 1A). In the zebrafish retinotectal pathway, all axons cross the midline at the chiasm to project to the contralateral optic tectum (Burrill and Easter, 1994). *sema3d*, a secreted semaphorin, is expressed in the ventral diencephalon from 16 hpf (Halloran et al., 1999) until at least 5 dpf, at which point all RGC axons have reached the tectum (Burrill and Easter, 1994; Karlstrom et al., 1996; Stuermer, 1988). Throughout the period when RGC growth cones cross the midline (approximately 36-48 hpf), *sema3d* is expressed by cells both anterior and posterior to the region of the forming chiasm (Fig. 1B) and by midline cells in the ventral diencephalon just dorsal to where the RGC axons cross (Fig. 1C). This expression pattern is maintained throughout visual pathway development, although by 5 dpf the *sema3d*-expressing cells dorsal to the axons have shifted slightly posterior because of tissue growth and shape changes (Fig. 1D). Thus, *sema3d* is expressed at the ventral midline throughout the development of the optic chiasm.

Neuropilins (Npns) are receptor components for class 3 semaphorins. In zebrafish, Npn1a and Npn2b are involved in at least some Sema3d-mediated axon guidance events (Wolman et al., 2004). We have previously shown that *npn1a*, *npn1b* and *npn2a* are expressed by RGCs throughout RGC axon extension (Liu et al., 2004), indicating that RGCs should be capable of responding to Sema3d encountered at the midline of the forming optic chiasm.

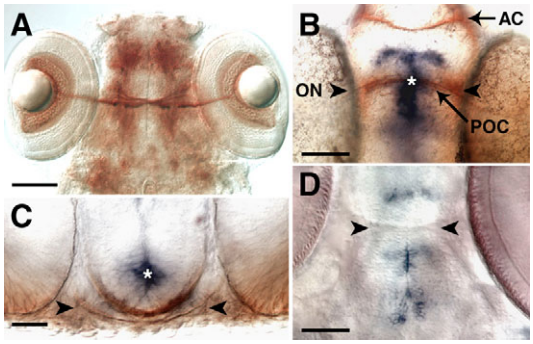

Fig. 1. *sema3d* is expressed at the midline of the ventral diencephalon throughout optic pathway development. A,B,D are ventral views with anterior up; C is a cross-section with dorsal up. (**A**) RGC axons labeled by Zn-5 immunohistochemistry at 5 dpf form the optic chiasm in the ventral diencephalon. (**B**,**C**) *sema3d* in situ hybridization (blue) and α-tubulin immunohistochemistry (brown) at 36 hpf (B) and 38 hpf (C) show *sema3d* expression at the midline of the ventral diencephalon, anterior, posterior and dorsal to where RGC axons cross the midline. (**D**) *sema3d* expression is maintained in the diencephalon through 5 dpf. Arrowheads show the location of RGC axons, and asterisks indicate the same region of *sema3d* in B and C. AC, anterior commissure; ON, optic nerve; POC, postoptic commissure. Scale bars: 100 μm in A; 50 μm in B,D; 25 μm in C.

RGC axons make ipsilateral guidance errors following global Sema3d expression

We first investigated whether Sema3d plays a role in the development of the optic chiasm by globally overexpressing *sema3d* in *Tg(hsp70:sema3d^{myc})* embryos, in which ubiquitous *sema3d* expression can be induced under the control of the zebrafish *hsp70* heat-shock promoter (Liu et al., 2004). *Tg(hsp70:sema3d^{myc})* embryos were heat shocked at 36, 42 and 48 hpf to induce Sema3d overexpression throughout RGC axon midline crossing, and were fixed at 5 dpf, after the tectum is innervated. Non-heat-shocked *Tg(hsp70:sema3d^{myc})* embryos and heat-shocked wild-type embryos were used to control for the presence of the transgene and the heat-shock treatment. RGC projections were visualized with unilateral DiI whole-eye fills.

Global Sema3d expression induced aberrant RGC projections to the ipsilateral tectum. At 5 dpf, dorsal imaging of tecta revealed ipsilateral projections in 97% (n=32) of Sema3d-overexpressing embryos but only 32% (n=25) of wild-type controls (P<0.000001; data not shown). Because the number of misguided axons varied between embryos, we also analyzed the extent of ipsilateral projections by calculating the percentage of ipsilateral tectal area covered by axons. Representative wild-type (Fig. 2A) and Sema3d-overexpressing (Fig. 2B,C) embryos are shown to illustrate the range of ipsilateral innervation observed. At 5 dpf, axons covered a significantly larger area of the ipsilateral tectum following Sema3d overexpression, an average of 11% of the tectal area, compared with 1-4% in control groups (Fig. 2E).

Ventral views of the optic chiasma of Sema3d-overexpressing embryos showed ipsilateral axons in the region of the optic tract (Fig. 2D). Analysis of individual confocal optical sections allowed us to trace these axons to the midline region, indicating that the axons projected to the midline before turning ipsilaterally. This observation suggests that ubiquitous Sema3d expression causes a specific axon guidance error at the chiasm midline to direct RGC axons into the ipsilateral optic tract.

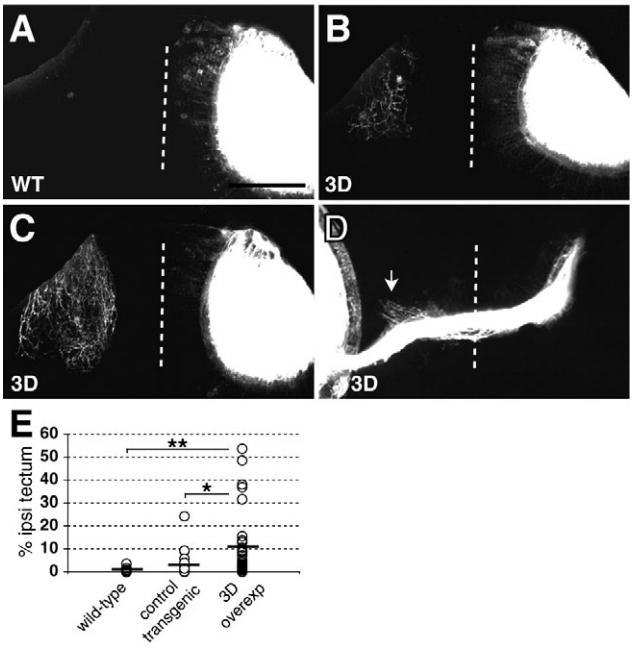

Fig. 2. Ubiquitous Sema3d overexpression increases aberrant ipsilateral projections. (**A-C**) Confocal projections of dorsal views of tecta in 5 dpf wild-type (A) and Sema3d-overexpressing (B,C) embryos show tectal innervation. Left eyes were injected and labeled eyes were digitally removed from images. Wild-type embryos (WT) contained few or no ipsilateral axons (A), whereas Sema3d-overexpressing embryos (3D) contained more extensive ipsilateral arbors (B,C). (**D**) Confocal projection of a ventral view of the optic chiasm in a 3 dpf Sema3d-overexpressing embryo, injected eye on the left, shows ipsilaterally projecting axons in the region of the optic tract (arrow). Ipsilateral axons are obscured near the midline by the labeled optic nerve in this projection. Dotted lines indicate midlines; anterior is up in all panels. Scale bars: 100 μm in A-C; 63 μm in D. (**E**) Scatter plot summarizing the extent of ipsilateral tectal innervation in each embryo at 5 dpf; lines indicate means. Sema3d overexpression significantly increased ipsilateral innervation at 5 dpf. WT, n=25; control transgenic embryos, n=20; Sema3d-overexpressing (3D overexp) embryos, n=32. *P<0.05, **P<0.02.

Live imaging reveals decreased RGC axon growth and increased pausing in the midline region following ubiquitous Sema3d expression

To gain insight into the mechanism by which Sema3d overexpression induces ipsilateral errors, we used timelapse imaging to analyze the behaviors of live RGC growth cones as they navigated their pathway. *Tg(hsp70:sema3d^{myc})* or wild-type embryos were injected with DiI into ventronasal or nasal retina at 34-38 hpf, heat shocked for one hour, and imaged for up to 14 hours. We analyzed rates of outgrowth, growth cone behaviors and growth cone morphology in three areas of the pathway: before growth cones reached the midline; in the midline region; and after leaving the midline region. (See Materials and methods for definitions of these regions.)

We found that global Sema3d expression selectively decreased RGC axon growth rate at the chiasm midline. Through the midline region, growth cones in Sema3d-overexpressing embryos advanced at only 7.7±1.9 μm/hour, which was significantly slower than control growth rates of 13.2±1.5 μm/hour (Fig. 3A, see also Movies 1 and 2 in the supplementary material). By contrast, outgrowth rates

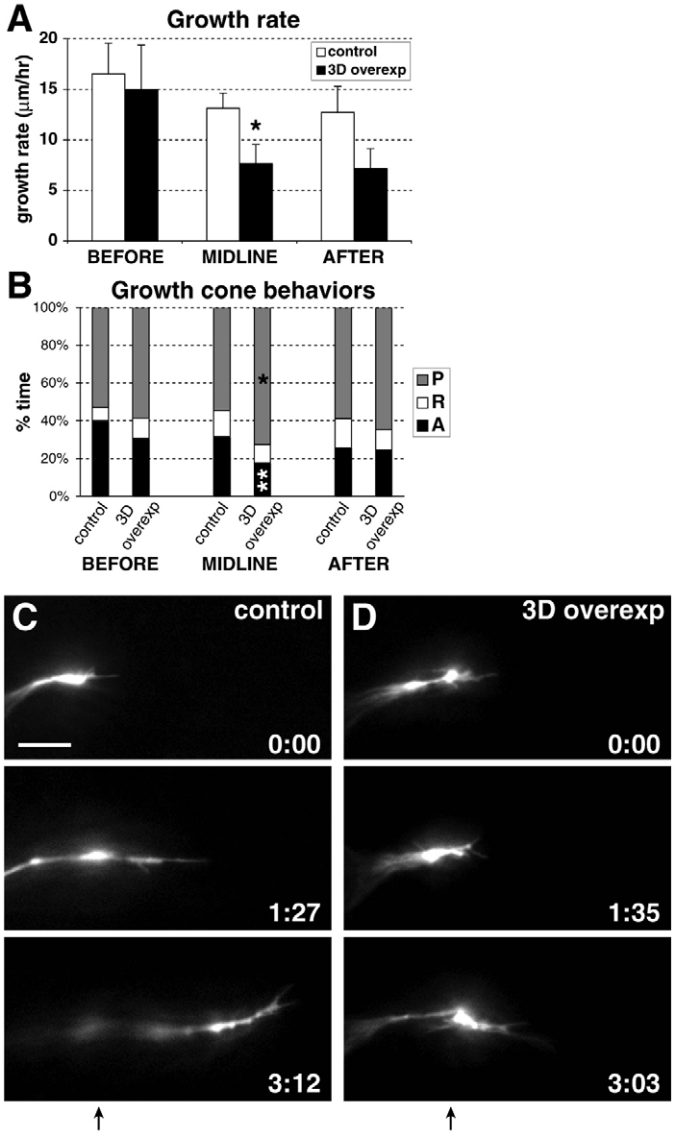

Fig. 3. Ubiquitous Sema3d overexpression slows midline growth by increasing growth cone pausing and decreasing growth cone advancing. (**A**) Overall growth rates in regions before, at and after the midline, reported as mean+s.e.m. Sema3d overexpression significantly decreased RGC growth rate in the midline region. Sema3d-overexpressing embryos, *n*=14 growth cones in 12 embryos; control embryos, *n*=2 growth cones in two wild-type embryos, 15 growth cones in 13 heat-shocked wild-type embryos, and two growth cones in two non-heat-shocked *Tg(hsp70:sema3d^{myc})* embryos. (**B**) Percentage of time growth cones spent advancing, pausing and retracting. Sema3d overexpression significantly increased time spent pausing and significantly decreased time spent advancing in the midline region. P, pausing; R, retracting; A, advancing. Sema3d-overexpressing embryos, *n*=15 growth cones in 12 embryos; control embryos, *n*=3 growth cones in two wild-type embryos, 15 growth cones in 12 heat-shocked wild-type embryos, and one growth cone in one non-heat-shocked *Tg(hsp70:sema3d^{myc})* embryo. *P<0.05; **P<0.02. (**C**,**D**) Frames taken from timelapse movies of growth cones in representative control (C) and Sema3d-overexpressing (D) embryos. Over a similar time period, the control growth cone extended from the midline into the optic tract, but the growth cone in the Sema3d-overexpressing embryo showed very limited forward growth. Times are indicated in hours:minutes; arrows below frame sequences indicate the midline. Anterior is up in all frames. Scale bar: 10 μm.

were not significantly changed by Sema3d overexpression either before or after the midline (Fig. 3A). Representative growth cones from control and Sema3d-overexpressing embryos are shown in Fig. 3. In just over three hours, this control growth cone extended from the midline well into the optic tract (Fig. 3C), whereas the growth cone in a Sema3d-overexpressing embryo remained near the midline (Fig. 3D).

To further investigate the growth cone behaviors underlying slowed growth, we calculated the percentage of time growth cones spent advancing, retracting and pausing. Again, RGC growth cones showed specific behavioral changes only at the midline in response to ubiquitous Sema3d. Within the midline region, Sema3d overexpression significantly decreased the percentage of time growth cones spent advancing (18±4%, compared with 32±3% in controls), and significantly increased the percentage of time growth cones were paused (73±6%, compared with 55±3% in controls; Fig. 3B). However, Sema3d overexpression did not affect growth cone retraction in this region, nor did it change any of the three behaviors either before or after the midline. Together, these findings demonstrate that RGC axons grew more slowly across the chiasm midline due to increased growth cone pausing and decreased advance. This live analysis also shows that RGC growth cones responded to ubiquitous Sema3d only while growing through the chiasm, suggesting that the responsiveness of these axons is tightly regulated and that they become sensitive to Sema3d only upon reaching the midline.

Ubiquitous Sema3d expression increases RGC growth cone complexity and axonal dynamics in the midline region

Our live analysis also revealed dramatic increases in RGC growth cone morphological and behavioral complexity at the midline in response to Sema3d overexpression. Consistent with previous studies (Bovolenta and Mason, 1987; Chan et al., 1998; Hutson and Chien, 2002; Mason and Erskine, 2000; Mason and Wang, 1997), control growth cones projecting toward the midline displayed a simple, streamlined shape with short filopodia extending from the leading edge of the growth cone (Fig. 4A, see Movie 1 in the supplementary material). Upon reaching the midline region, control growth cones became more complex with multiple filopodia extended toward the contralateral side (Fig. 4B). Before the midline, growth cones in Sema3d-overexpressing embryos also had simple morphologies, and were indistinguishable from control growth cones (Fig. 4C). Upon reaching the midline region, these growth cones exhibited a larger increase in morphological complexity than control growth cones, extending longer filopodia in multiple directions, including back towards the ipsilateral side (Fig. 4D, see Movie 2 in the supplementary material). Growth cones in three Sema3d-overexpressing embryos exhibited an extremely complex morphology, with long and active filopodia projecting in all directions (Fig. 4E,F, see also Movie 3 in the supplementary material). These growth cones remained stalled near the midline for 6-11 hours, spending more than 90% of their time paused and with overall growth rates of 0 μm/hour. Some of the filopodia of these growth cones also had unusually long lifetimes, with individual processes persisting for up to five hours.

The axon shafts proximal to the growth cones also responded to Sema3d overexpression with dynamic morphological changes, shifting to form convoluted trajectories (Fig. 4G). These axon movements occurred in 33% (*n*=15) of Sema3d-overexpressing embryos, but in only 15% (*n*=20) of control embryos. Axon movements in Sema3d-overexpressing embryos were also larger and

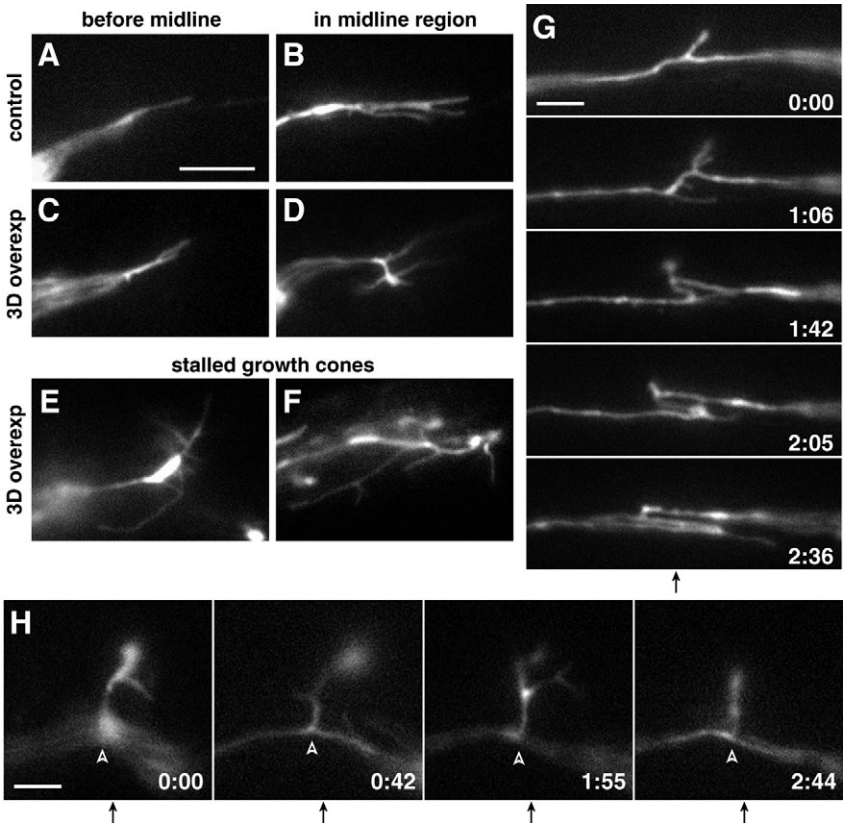

Fig. 4. Live imaging reveals increased growth cone complexity and axonal dynamics following ubiquitous Sema3d expression. (**A-D**) Single frames from timelapse movies show representative RGC growth cone morphology in wild-type (A,B) and Sema3d-overexpressing (C,D) embryos before and at the midline. Sema3d overexpression did not affect morphology before growth cones reached the midline but increased complexity in the midline region. (**E**,**F**) Stalled growth cones in Sema3d-overexpressing embryos showed extremely complex morphology. (**G**,**H**) Frames taken from timelapse movies of Sema3d-overexpressing embryos show examples of (G) dynamic axonal movements and (H) an interstitial projection (arrowheads) from the midline. Times are reported in hours:minutes; midlines are indicated by arrows below frame sequences. Anterior is up in all frames. Scale bars: 10 μm in A-F; 5 μm in G,H.

continued for longer periods of time than did those in controls, and suggest that exposure to ubiquitous Sema3d may alter adhesion of the axons or their substrate. Axons also extended interstitial filopodium-like processes that occurred along 86% (n=14) of axons in Sema3d-overexpressing embryos, but along only 25% (n=20) of axons in control embryos. These processes emerged along all regions of the axon but were most numerous and persistent at the midline (Fig. 4H).

These findings show that RGC axons respond to global Sema3d expression with increased growth cone and axonal complexity, and prolonged stalling at the chiasm midline. Complex growth cone morphology has previously been associated with pausing and exploratory behavior (Bovolenta and Mason, 1987; Chan et al., 1998; Mason and Wang, 1997), suggesting that exposure to ubiquitous Sema3d may cause RGC axons to pause at the midline and search for guidance information.

Sema3d knockdown induces ipsilateral RGC axon guidance errors and reduces midline crossing

In addition to Sema3d overexpression, we examined the effect of loss-of-function on RGC projections, as a more specific test of Sema3d function. We used a morpholino antisense knockdown approach with a morpholino oligonucleotide that has been previously shown to block Sema3d translation (Liu et al., 2004; Wolman et al., 2004). We injected morpholinos into newly fertilized embryos (see Materials and methods for doses), and fixed embryos at 2.5, 3.5 or 5 dpf.

RGC axons in Sema3d morphant (morpholino-injected) embryos showed three primary axon phenotypes. First, as in Sema3d-overexpressing embryos, a subset of axons turned ipsilaterally instead of crossing the chiasm midline and extended in the region of the ipsilateral optic tract (arrows, Fig. 5D-F,I). In ventral images of the chiasm region, ipsilateral guidance errors were visible in significantly more Sema3d knockdown embryos than control embryos at all three ages examined (Fig. 5J). With all ages combined, ipsilateral projections in the chiasm region occurred in 56% of Sema3d morphants, but in only 10% of embryos injected with a four-base mismatch control morpholino. The ipsilateral phenotype was also stronger in Sema3d morphants, which frequently had several turning axons (Fig. 5F,I), whereas control morpholino-injected embryos typically had only one ipsilateral axon.

Second, some RGC axons turned and extended anteriorly from the correct pathway (arrowheads, Fig. 5D,F). This type of guidance error was not seen following Sema3d overexpression. At 2.5 dpf, anterior projections occurred in 25% of Sema3d morpholino-injected embryos but were not seen in control embryos (Fig. 5J). Interestingly, at later ages, anterior projections occurred at similar low frequencies of 7-23% in both control and Sema3d morphant embryos.

Third, Sema3d knockdown reduced the midline crossing of RGC axons. RGC axon bundles crossed the chiasm midline in all control embryos at 2.5 dpf, but reached the midline in only 82% of Sema3d morphant embryos at the same age (Fig. 5J); this suggests that RGC axon growth may be delayed in the absence of Sema3d. Within axon bundles that did reach the midline by 2.5 dpf, growth cones were visible at the midline in 52% of Sema3d morphants (Fig. 5G), but in only 10% of controls, indicating that Sema3d knockdown may increase growth cone pausing or stalling at the midline, as was seen in the timelapse movies of Sema3d-overexpressing embryos. Similar results were found at 3.5 dpf (Fig. 5J). In some cases, large numbers of axons extended to the midline but failed to extend beyond it (Fig. 5H), further suggesting that Sema3d knockdown induces pausing or stalling at the midline. Sema3d morphants had noticeably smaller

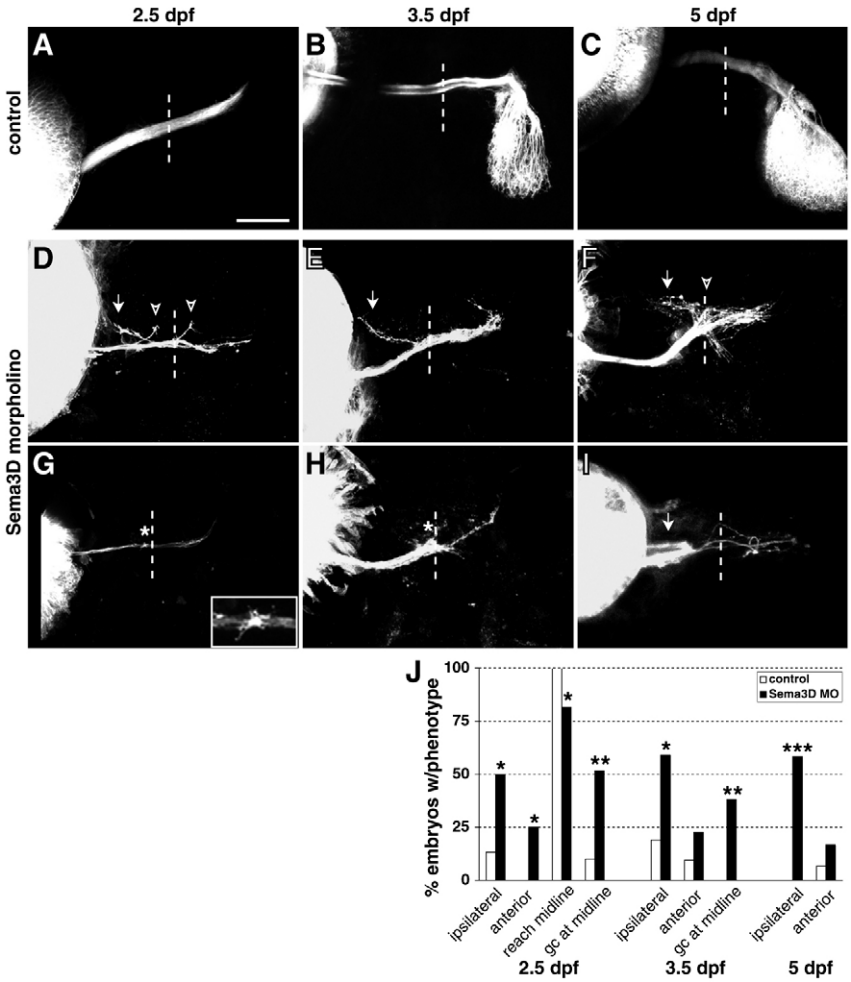

Fig. 5. Sema3d knockdown increases ipsilateral guidance errors and reduces midline crossing. (A-I) Confocal projections of DiI-labeled RGC axons in control (**A-C**) or Sema3d (**D-I**) morpholino-injected embryos at 2.5 (A,D,G), 3.5 (B,E,H) and 5 (C,F,I) dpf; injected eyes are on the left. A,D-I are ventral views; B and C are dorsal views. Sema3d knockdown caused aberrant projections ipsilaterally (arrows) and anteriorly (arrowheads) from the normal pathway, and increased the occurrence of axons extending to but not beyond the midline (asterisks). Inset in G shows an enlargement of a growth cone near midline. Dotted lines indicate midlines; anterior is up in all panels. Scale bars: 50 μm in A,D-I; 80 μm in B,C. (**J**) Summary of guidance and extension errors following Sema3d morpholino (Sema3d MO) knockdown. At 2.5 dpf: control morpholino, *n*=30 for all analyses; Sema3d morpholino, *n*=38 analyzed for reaching the midline, *n*=31 analyzed for presence of growth cones, *n*=28 analyzed for guidance errors. At 3.5 dpf: control morpholino, *n*=21; Sema3d morpholino, *n*=22. At 5 dpf: control morpholino, *n*=30; Sema3d morpholino, *n*=36. **P*<0.01; ***P*<0.001; ****P*<0.000001.

RGC axon bundles at all ages, and a small number of DiI eye fills did not label any axons, indicating that Sema3d knockdown may occasionally reduce or severely delay RGC axon outgrowth.

These results show that Sema3d loss-of-function decreases the extension of RGC projections beyond the chiasm midline. Aberrant anterior projections imply a loss of repulsion anterior to the chiasm, suggesting that Sema3d normally prohibits RGC axon extension into this area. Similar to global Sema3d overexpression, Sema3d knockdown also increases the incidence of ipsilateral turning errors at the midline, suggesting that Sema3d is normally involved in guiding RGC axons across the midline and into the contralateral optic tract.

Timelapse imaging reveals increased midline pausing and aberrant projections following Sema3d knockdown

We used live timelapse imaging to examine how Sema3d knockdown affects RGC growth cone behavior to generate guidance errors. Growth cones or axons were imaged in 23 Sema3d morphant embryos for up to 23 hours with *z*-stacks collected every 2 minutes.

In the region before the midline, RGC growth cones in Sema3d morphant embryos maintained a simple morphology (data not shown), similar to growth cones in both control and Sema3d-overexpressing embryos. Interestingly, 42% (*n*=12) of growth cones imaged before the midline paused briefly (30-90 minutes) just before reaching the midline. From the midline onward, growth cones in Sema3d morpholino-injected embryos (*n*=16) displayed three behaviors not seen in controls (Fig. 6A). First, 44% of growth cones crossed the midline then paused in the proximal optic tract throughout the remainder of the imaging session (2-8 hours). Similar to the stalling behavior caused by Sema3d overexpression, these long pauses were characterized by shape changes, increased morphological complexity, and dynamic filopodial extensions and retractions. However, unlike growth cone stalling in Sema3d-overexpressing embryos, these long pauses were separated by brief periods of forward growth. Second, 25% of growth cones in Sema3d morphants repeatedly advanced and retracted between the midline and the proximal optic tract (Fig. 6B, see Movie 4 in the supplementary material). Periods of extension and retraction were separated by pauses, and these growth cones made no net forward progress despite being extremely active. Third, another 13% of growth cones engaged in repeated extensions and retractions after crossing the midline but still made slow progress along the optic tract. This increased incidence of growth cone retractions distinguished Sema3d knockdown from Sema3d overexpression, which, as discussed earlier, did not change the frequency of growth cone retractions. The final 19% of growth cones grew across the midline and extended into the dorsal optic tract with no unusual pausing or retractions.

Sema3d knockdown also increased the incidence of interstitial projections along RGC axon shafts similar to those caused by Sema3d overexpression. Projections occurred in 74% (*n*=23) of

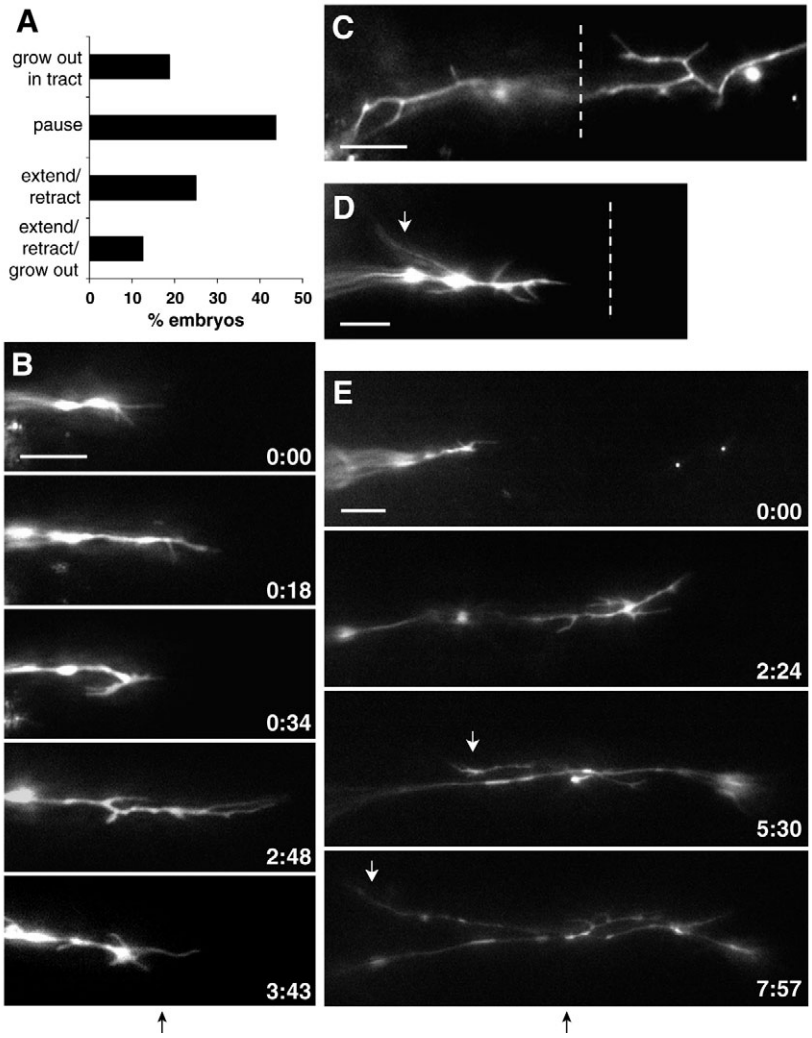

Fig. 6. RGC axons show ipsilateral and interstitial projections and reduced growth beyond the midline following Sema3d knockdown. (**A**) Summary of growth cone behaviors after reaching the chiasm midline in Sema3d morphant embryos. (**B**) Frames taken from a timelapse movie of a Sema3d morphant embryo show repeated growth cone extensions and retractions at the midline. (**C**,**D**) Sema3d knockdown induced interstitial processes, including ipsilateral projections (white arrow). (**E**) Some processes developed into ipsilateral growth cones (white arrows). Times are indicated in hours:minutes; midlines are indicated by dotted lines or black arrows below frame sequences. Anterior is up in all frames. Scale bars: 10 μm.

Sema3d morphant embryos, compared with 25% of control axons (described in overexpression experiments). These projections were very active and emerged from all regions of the axon to project anteriorly or posteriorly from the pathway (Fig. 6C). Anterior projections arising near the midline were the most complex, dynamic and persistent, and frequently included processes directed back toward the midline or ipsilateral side (Fig. 6C, see Movie 5 in the supplementary material). Other anterior projections extended in the region of the ipsilateral optic tract; these processes arose both from axons whose growth cones had already extended into the contralateral optic tract and from axons whose growth cones were still approaching the midline (Fig. 6D). In two embryos, anterior interstitial projections developed into new growth cones that appeared to extend in the ipsilateral optic tract (Fig. 6E, see Movie 6 in the supplementary material). Ipsilateral growth cones were imaged in a total of 26% of Sema3d morphant embryos. Interestingly, some of the ipsilateral projections, including the two de novo ipsilateral growth cones, appeared to emerge from axons that had growth cones simultaneously extending in the contralateral optic tract (Fig. 6E, Movie 6 in the supplementary material). Although RGC axons have never been described to branch in the optic chiasm, these movies suggest that individual axons might extend growth cones to both sides of the brain following Sema3d knockdown. It remains to be seen whether a single axon can maintain bilateral projections or if one projection will retract in favor of the other. Alternatively, from our analysis, we cannot rule out the possibility that the simultaneously imaged ipsilateral and contralateral growth cones arose from separate but very tightly apposed axons.

These observations show that Sema3d knockdown increased RGC growth cone pausing and retraction behavior around the chiasm midline, impairing the ability of growth cones to extend away from the midline into the optic tract. Loss of Sema3d function simultaneously increased morphological complexity and axonal processes, suggesting that Sema3d knockdown, like ubiquitous Sema3d overexpression, increases growth cone exploratory behavior. Together with the specific guidance errors observed in fixed Sema3d morphants, these findings suggest that Sema3d normally provides a directional guidance cue at the midline to promote RGC axon extension from the midline into the contralateral optic tract.

DISCUSSION

In this study, we show that Sema3d plays an important role in guiding the midline crossing decision of RGC axons during formation of the optic chiasm. Global Sema3d expression or knockdown caused RGC axons to project to the ipsilateral optic tectum in a species whose visual pathway is normally entirely crossed. Live imaging revealed that ubiquitous Sema3d slowed RGC axon growth rates and increased growth cone pausing and

complexity at the chiasm midline, whereas Sema3d knockdown caused repeated growth cone retraction or pausing, and impaired the ability of RGC axons to leave the midline region. Both manipulations reduced midline crossing of RGC axons, suggesting that Sema3d normally directs RGC axons across the chiasm midline and into the contralateral optic tract.

Our data support a model in which RGC axons encounter Sema3d at the midline of the ventral diencephalon and are repelled down a gradient away from the midline and into the contralateral optic tract. This proposed model has three independent requirements: (1) RGC axons respond to Sema3d as a repulsive cue; (2) RGC axons become responsive to Sema3d upon reaching the midline; and (3) RGC axons derive directional information from a gradient of Sema3d expression.

First, changes in RGC axon outgrowth and behavior following Sema3d manipulation strongly suggest that RGC axons are repelled by Sema3d. Sema3d knockdown impaired the ability of growth cones to leave the midline, which was revealed through live analysis to be caused by either intermittent advance or repeated extension and retraction. These growth cone behaviors could indicate that Sema3d knockdown caused the loss of either a repulsive signal propelling axons away from the midline or a permissive signal allowing axon advance through the midline region. However, RGC axons in Sema3d morphants also extended aberrant processes into the anterior region of normal Sema3d expression, suggesting that Sema3d normally inhibits growth into these areas. A repulsive role of Sema3d is also consistent with previous work in our laboratory showing that RGC growth cones were inhibited or repelled by localized ectopic patches of Sema3d near the optic tract (Liu et al., 2004). Effects observed after ubiquitous Sema3d overexpression, including slowed growth and increased growth cone pausing in the midline region, are not consistent with a simple permissive role of Sema3d but could be indicative of increased inhibition. Finally, increased interstitial projections following Sema3d overexpression may reflect a repellent environment; this is supported by in vitro studies showing that RGC axons undergo extensive back-branching after growth cone collapse in response to both uniform application and point sources of known repellent cues (Campbell et al., 2001; Davenport et al., 1999). Together, our findings are most consistent with a role for Sema3d as a repulsive cue for RGC axons.

Second, our findings suggest that RGC axons become sensitive to Sema3d-mediated repulsion only after reaching the chiasm midline. Normally, RGC growth cones first encounter Sema3d at the midline, implying that the Sema3d expression pattern could determine the onset of responsiveness. However, even in Sema3d-overexpressing embryos, in which RGC axons grow through Sema3d-expressing tissues before the midline, RGC growth cones showed no significant behavioral or guidance responses to the ubiquitous Sema3d until they reached the midline region. Both Sema3d overexpression and knockdown caused dramatic increases in growth cone exploratory behavior at the midline, suggesting the disruption of guidance information normally used by the growth cones in this region. Interestingly, although all phenotypes indicative of repulsion occurred at the midline, our proposed model does not exclude the possibility that Sema3d may also play some role in promoting RGC axon growth to the midline. Some Sema3d morphant embryos showed delayed or reduced RGC axon outgrowth or brief growth cone pausing before the midline. If Sema3d does help to attract axons to the midline, our findings indicate that RGC axons must then switch their responsiveness to Sema3d from attraction to repulsion upon crossing the midline.

Midline axon guidance is inherently asymmetric, requiring axons to approach then leave the same tissue, and studies of other midline systems show precedence for changes in growth cone responsiveness at the midline. Commissural axons in *Drosophila* ventral nerve cord and vertebrate spinal cord and hindbrain are initially attracted to midline Netrin, but lose this responsiveness after reaching the midline and become repelled by midline Slit to extend to the contralateral side (Harris et al., 1996; Kennedy et al., 1994; Kidd et al., 1999; Kidd et al., 1998a; Kidd et al., 1998b; Mitchell et al., 1996; Shirasaki et al., 1998; Shirasaki and Murakami, 2001; Zou et al., 2000). RGC axons are also capable of regulating their guidance responses; in *Xenopus*, RGC axons acquire sensitivity to Sema3a as a repellent after crossing the chiasm midline (Campbell et al., 2001). Alternatively, cells can change the nature of their response to a single cue. For example, migrating mesoderm cells in *Drosophila* switch their response to Slit from repulsion to attraction at different points in their pathway (Kramer et al., 2001). Similarly, *Xenopus* RGC axons are attracted to Netrin as they exit the eye, lose responsiveness to Netrin as they cross the midline, and become repelled by Netrin as they approach the optic tectum (Shewan et al., 2002). Both sensitivity and modality of growth cone responses to particular cues can be modulated by a number of factors, including expression levels of specific receptor components (Hong et al., 1999; Julien et al., 2005; Keleman et al., 2002; Wolman et al., 2004), activation of other surface molecules (Hopker et al., 1999; Kantor et al., 2004; Sabatier et al., 2004; Stein and Tessier-Lavigne, 2001; Stoeckli et al., 1997), and levels of intracellular signaling molecules such as cyclic nucleotides (Polleux et al., 2000; Song et al., 1998; Song et al., 1997), indicating that both intrinsic and extrinsic factors are probably involved in determining how RGC growth cones respond to midline Sema3d.

Third, our results support the hypothesis that RGC growth cones rely on a gradient of Sema3d to provide the directional information needed to guide projections contralaterally. Global Sema3d overexpression and knockdown both alter the normal midline pattern of Sema3d expression. Likewise, the two Sema3d manipulations resulted in many similar midline axon phenotypes, including ipsilateral projections, growth cone pausing and increased morphological complexity. These phenotypes indicate that Sema3d-mediated guidance information was lost at the midline following both overexpression and knockdown, demonstrating that the presence or absence of Sema3d is not sufficient to convey guidance information but that the correct pattern of expression is also needed. Although the majority of RGC axons were eventually able to extend away from the midline despite changes in midline cues, the formation of ipsilateral projections suggests that the directionality of this guidance decision was impaired. RGC axons are known to use gradients of guidance cues, including Sema3d and others, for retinotopic mapping on the surface of the optic tectum or superior colliculus (McLaughlin and O'Leary, 2005). The importance of gradients for proper RGC guidance in the tectum further suggests that cue gradients may also be important for guidance at the midline.

Together, our findings show that midline Sema3d plays an important role in the development of the contralateral visual pathway. Our model does not exclude the possibility that Sema3d may act in concert with other guidance factors. For example, some guidance effects of Sema3a and Sema3b are mediated by receptor complexes formed by neuropilins and immunoglobulin superfamily cell adhesion molecules (Sema3a by Npn1 with L1, and Sema3b by Npn2 with NrCAM) (Castellani et al., 2000; Castellani et al., 2002; Falk et al., 2005). Additionally, many RGC axons still cross the midline after our manipulations of Sema3d, indicating that Sema3d

is probably not the only factor directing RGC laterality in the zebrafish. Several zebrafish mutants with ipsilateral guidance errors were identified in a large-scale mutagenesis screen (Karlstrom et al., 1996). Many of these mutations affect patterning and development of the diencephalon midline, suggesting that they may influence guidance cues indirectly. Interestingly, in a Gli2 mutant, *yot*, midline *sema3d* expression is reduced or absent in the ventral diencephalon, and both RGC axons and those of another ventral commissure, the postoptic commissure, fail to cross the midline (Barresi et al., 2005; Karlstrom et al., 1996). Further analysis of these mutants may identify other cues important for laterality of RGC projections during formation of the optic chiasm.

Live imaging of RGC axons and growth cones in combination with manipulations of a putative guidance factor, Sema3d, demonstrates how live cell behaviors can elucidate the nature and mechanisms of guidance cue function in vivo. Here, disruption of the normal Sema3d expression pattern in the ventral diencephalon through global overexpression or knockdown caused phenotypes that appear very similar in fixed embryos, but which can be distinguished through differences in growth cone behaviors and dynamics. These experiments have allowed us to identify Sema3d as an important extrinsic cue for guiding the midline crossing of RGC axons to develop the correct laterality of the zebrafish visual system.

The authors wish to thank members of the Halloran lab, Dr Timothy Gomez and Dr Katherine Kalil for comments on the manuscript. Some materials used were provided by the Zebrafish International Research Center, supported by NIH-NCRR P40 RR12546. This work was funded by a Howard Hughes Medical Institute Predoctoral Fellowship to J.A.S. and by NINDS NS42228 to M.C.H.

Supplementary material

Supplementary material for this article is available at
http://dev.biologists.org/cgi/content/full/133/6/1035/DC1

References

Barresi, M. J., Hutson, L. D., Chien, C. B. and Karlstrom, R. O. (2005). Hedgehog regulated Slit expression determines commissure and glial cell position in the zebrafish forebrain. *Development* **132**, 3643-3656.

Bovolenta, P. and Mason, C. (1987). Growth cone morphology varies with position in the developing mouse visual pathway from retina to first targets. *J. Neurosci.* **7**, 1447-1460.

Burrill, J. D. and Easter, S. S., Jr (1994). Development of the retinofugal projections in the embryonic and larval zebrafish (Brachydanio rerio). *J. Comp. Neurol.* **346**, 583-600.

Campbell, D. S., Regan, A. G., Lopez, J. S., Tannahill, D., Harris, W. A. and Holt, C. E. (2001). Semaphorin 3A elicits stage-dependent collapse, turning, and branching in Xenopus retinal growth cones. *J. Neurosci.* **21**, 8538-8547.

Castellani, V., Chedotal, A., Schachner, M., Faivre-Sarrailh, C. and Rougon, G. (2000). Analysis of the L1-deficient mouse phenotype reveals cross-talk between Sema3A and L1 signaling pathways in axonal guidance. *Neuron* **27**, 237-249.

Castellani, V., De Angelis, E., Kenwrick, S. and Rougon, G. (2002). Cis and trans interactions of L1 with neuropilin-1 control axonal responses to semaphorin 3A. *EMBO J.* **21**, 6348-6357.

Chan, S. O., Wong, K. F., Chung, K. Y. and Yung, W. H. (1998). Changes in morphology and behaviour of retinal growth cones before and after crossing the midline of the mouse chiasm – a confocal microscopy study. *Eur. J. Neurosci.* **10**, 2511-2522.

Chung, K. Y., Taylor, J. S., Shum, D. K. and Chan, S. O. (2000). Axon routing at the optic chiasm after enzymatic removal of chondroitin sulfate in mouse embryos. *Development* **127**, 2673-2683.

Cox, K. H., DeLeon, D. V., Angerer, L. M. and Angerer, R. C. (1984). Detection of mrnas in sea urchin embryos by in situ hybridization using asymmetric RNA probes. *Dev. Biol.* **101**, 485-502.

Davenport, R. W., Thies, E. and Cohen, M. L. (1999). Neuronal growth cone collapse triggers lateral extensions along trailing axons. *Nat. Neurosci.* **2**, 254-259.

Erskine, L., Williams, S. E., Brose, K., Kidd, T., Rachel, R. A., Goodman, C. S., Tessier-Lavigne, M. and Mason, C. A. (2000). Retinal ganglion cell axon guidance in the mouse optic chiasm: expression and function of robos and slits. *J. Neurosci.* **20**, 4975-4982.

Falk, J., Bechara, A., Fiore, R., Nawabi, H., Zhou, H., Hoyo-Becerra, C., Bozon, M., Rougon, G., Grumet, M., Puschel, A. W. et al. (2005). Dual functional activity of semaphorin 3B is required for positioning the anterior commissure. *Neuron* **48**, 63-75.

Godement, P., Wang, L. C. and Mason, C. A. (1994). Retinal axon divergence in the optic chiasm: dynamics of growth cone behavior at the midline. *J. Neurosci.* **14**, 7024-7039.

Halloran, M. C., Severance, S. M., Yee, C. S., Gemza, D. L., Raper, J. A. and Kuwada, J. Y. (1999). Analysis of a Zebrafish semaphorin reveals potential functions in vivo. *Dev. Dyn.* **214**, 13-25.

Harris, R., Sabatelli, L. M. and Seeger, M. A. (1996). Guidance cues at the Drosophila CNS midline: identification and characterization of two Drosophila Netrin/UNC-6 homologs. *Neuron* **17**, 217-228.

Herrera, E., Brown, L., Aruga, J., Rachel, R. A., Dolen, G., Mikoshiba, K., Brown, S. and Mason, C. A. (2003). Zic2 patterns binocular vision by specifying the uncrossed retinal projection. *Cell* **114**, 545-557.

Herrera, E., Marcus, R., Li, S., Williams, S. E., Erskine, L., Lai, E. and Mason, C. (2004). Foxd1 is required for proper formation of the optic chiasm. *Development* **131**, 5727-5739.

Hong, K., Hinck, L., Nishiyama, M., Poo, M. M., Tessier-Lavigne, M. and Stein, E. (1999). A ligand-gated association between cytoplasmic domains of UNC5 and DCC family receptors converts netrin-induced growth cone attraction to repulsion. *Cell* **97**, 927-941.

Hopker, V. H., Shewan, D., Tessier-Lavigne, M., Poo, M. and Holt, C. (1999). Growth-cone attraction to netrin-1 is converted to repulsion by laminin-1. *Nature* **401**, 69-73.

Hutson, L. D. and Chien, C. B. (2002). Pathfinding and error correction by retinal axons: the role of astray/robo2. *Neuron* **33**, 205-217.

Kantor, D. B., Chivatakarn, O., Peer, K. L., Oster, S. F., Inatani, M., Hansen, M. J., Flanagan, J. G., Yamaguchi, Y., Sretavan, D. W., Giger, R. J. et al. (2004). Semaphorin 5A is a bifunctional axon guidance cue regulated by heparan and chondroitin sulfate proteoglycans. *Neuron* **44**, 961-975.

Karlstrom, R. O., Trowe, T., Klostermann, S., Baier, H., Brand, M., Crawford, A. D., Grunewald, B., Haffter, P., Hoffmann, H., Meyer, S. U. et al. (1996). Zebrafish mutations affecting retinotectal axon pathfinding. *Development* **123**, 427-438.

Keleman, K., Rajagopalan, S., Cleppien, D., Teis, D., Paiha, K., Huber, L. A., Technau, G. M. and Dickson, B. J. (2002). Comm sorts robo to control axon guidance at the Drosophila midline. *Cell* **110**, 415-427.

Kennedy, T. E., Serafini, T., de la Torre, J. R. and Tessier-Lavigne, M. (1994). Netrins are diffusible chemotropic factors for commissural axons in the embryonic spinal cord. *Cell* **78**, 425-435.

Kidd, T., Brose, K., Mitchell, K. J., Fetter, R. D., Tessier-Lavigne, M., Goodman, C. S. and Tear, G. (1998a). Roundabout controls axon crossing of the CNS midline and defines a novel subfamily of evolutionarily conserved guidance receptors. *Cell* **92**, 205-215.

Kidd, T., Russell, C., Goodman, C. S. and Tear, G. (1998b). Dosage-sensitive and complementary functions of roundabout and commissureless control axon crossing of the CNS midline. *Neuron* **20**, 25-33.

Kidd, T., Bland, K. S. and Goodman, C. S. (1999). Slit is the midline repellent for the robo receptor in Drosophila. *Cell* **96**, 785-794.

Kimmel, C. B., Ballard, W. W., Kimmel, S. R., Ullmann, B. and Schilling, T. F. (1995). Stages of embryonic development of the zebrafish. *Dev. Dyn.* **203**, 253-310.

Kramer, S. G., Kidd, T., Simpson, J. H. and Goodman, C. S. (2001). Switching repulsion to attraction: changing responses to slit during transition in mesoderm migration. *Science* **292**, 737-740.

Lin, L. and Chan, S. O. (2003). Perturbation of CD44 function affects chiasmatic routing of retinal axons in brain slice preparations of the mouse retinofugal pathway. *Eur. J. Neurosci.* **17**, 2299-2312.

Liu, Y., Berndt, J., Su, F., Tawarayama, H., Shoji, W., Kuwada, J. Y. and Halloran, M. C. (2004). Semaphorin3D guides retinal axons along the dorsoventral axis of the tectum. *J. Neurosci.* **24**, 310-318.

Mason, C. and Erskine, L. (2000). Growth cone form, behavior, and interactions in vivo: retinal axon pathfinding as a model. *J. Neurobiol.* **44**, 260-270.

Mason, C. A. and Wang, L. C. (1997). Growth cone form is behavior-specific and, consequently, position-specific along the retinal axon pathway. *J. Neurosci.* **17**, 1086-1100.

McLaughlin, T. and O'Leary, D. D. (2005). Molecular gradients and development of retinotopic maps. *Annu. Rev. Neurosci.* **28**, 327-355.

Mitchell, K. J., Doyle, J. L., Serafini, T., Kennedy, T. E., Tessier-Lavigne, M., Goodman, C. S. and Dickson, B. J. (1996). Genetic analysis of Netrin genes in Drosophila: Netrins guide CNS commissural axons and peripheral motor axons. *Neuron* **17**, 203-215.

Nakagawa, S., Brennan, C., Johnson, K. G., Shewan, D., Harris, W. A. and Holt, C. E. (2000). Ephrin-B regulates the Ipsilateral routing of retinal axons at the optic chiasm. *Neuron* **25**, 599-610.

Nasevicius, A. and Ekker, S. C. (2000). Effective targeted gene 'knockdown' in zebrafish. *Nat. Genet.* **26**, 216-220.

Pak, W., Hindges, R., Lim, Y. S., Pfaff, S. L. and O'Leary, D. D. (2004). Magnitude of binocular vision controlled by islet-2 repression of a genetic program that specifies laterality of retinal axon pathfinding. *Cell* **119**, 567-578.

Plump, A. S., Erskine, L., Sabatier, C., Brose, K., Epstein, C. J., Goodman, C. S., Mason, C. A. and Tessier-Lavigne, M. (2002). Slit1 and Slit2 cooperate to prevent premature midline crossing of retinal axons in the mouse visual system. *Neuron* **33**, 219-232.

Polleux, F., Morrow, T. and Ghosh, A. (2000). Semaphorin 3A is a chemoattractant for cortical apical dendrites. *Nature* **404**, 567-573.

Pratt, T., Tian, N. M., Simpson, T. I., Mason, J. O. and Price, D. J. (2004). The winged helix transcription factor Foxg1 facilitates retinal ganglion cell axon crossing of the ventral midline in the mouse. *Development* **131**, 3773-3784.

Ringstedt, T., Braisted, J. E., Brose, K., Kidd, T., Goodman, C., Tessier-Lavigne, M. and O'Leary, D. D. (2000). Slit inhibition of retinal axon growth and its role in retinal axon pathfinding and innervation patterns in the diencephalon. *J. Neurosci.* **20**, 4983-4991.

Sabatier, C., Plump, A. S., Le, M., Brose, K., Tamada, A., Murakami, F., Lee, E. Y. and Tessier-Lavigne, M. (2004). The divergent Robo family protein rig-1/Robo3 is a negative regulator of slit responsiveness required for midline crossing by commissural axons. *Cell* **117**, 157-169.

Shewan, D., Dwivedy, A., Anderson, R. and Holt, C. E. (2002). Age-related changes underlie switch in netrin-1 responsiveness as growth cones advance along visual pathway. *Nat. Neurosci.* **5**, 955-962.

Shirasaki, R. and Murakami, F. (2001). Crossing the floor plate triggers sharp turning of commissural axons. *Dev. Biol.* **236**, 99-108.

Shirasaki, R., Katsumata, R. and Murakami, F. (1998). Change in chemoattractant responsiveness of developing axons at an intermediate target. *Science* **279**, 105-107.

Song, H. J., Ming, G. L. and Poo, M. M. (1997). cAMP-induced switching in turning direction of nerve growth cones. *Nature* **388**, 275-279.

Song, H., Ming, G., He, Z., Lehmann, M., McKerracher, L., Tessier-Lavigne, M. and Poo, M. (1998). Conversion of neuronal growth cone responses from repulsion to attraction by cyclic nucleotides. *Science* **281**, 1515-1518.

Sretavan, D. W. and Reichardt, L. F. (1993). Time-lapse video analysis of retinal ganglion cell axon pathfinding at the mammalian optic chiasm: growth cone guidance using intrinsic chiasm cues. *Neuron* **10**, 761-777.

Stein, E. and Tessier-Lavigne, M. (2001). Hierarchical organization of guidance receptors: silencing of netrin attraction by slit through a Robo/DCC receptor complex. *Science* **291**, 1928-1938.

Stoeckli, E. T., Sonderegger, P., Pollerberg, G. E. and Landmesser, L. T. (1997). Interference with axonin-1 and NrCAM interactions unmasks a floor-plate activity inhibitory for commissural axons. *Neuron* **18**, 209-221.

Stuermer, C. A. (1988). Retinotopic organization of the developing retinotectal projection in the zebrafish embryo. *J. Neurosci.* **8**, 4513-4530.

Wang, L. C., Dani, J., Godement, P., Marcus, R. C. and Mason, C. A. (1995). Crossed and uncrossed retinal axons respond differently to cells of the optic chiasm midline in vitro. *Neuron* **15**, 1349-1364.

Williams, S. E., Mann, F., Erskine, L., Sakurai, T., Wei, S., Rossi, D. J., Gale, N. W., Holt, C. E., Mason, C. A. and Henkemeyer, M. (2003). Ephrin-B2 and EphB1 mediate retinal axon divergence at the optic chiasm. *Neuron* **39**, 919-935.

Wolman, M. A., Liu, Y., Tawarayama, H., Shoji, W. and Halloran, M. C. (2004). Repulsion and attraction of axons by semaphorin3D are mediated by different neuropilins in vivo. *J. Neurosci.* **24**, 8428-8435.

Zou, Y., Stoeckli, E., Chen, H. and Tessier-Lavigne, M. (2000). Squeezing axons out of the gray matter: a role for slit and semaphorin proteins from midline and ventral spinal cord. *Cell* **102**, 363-375.